IOP Publishing Smart Materials and Structures
Smart Mater. Struct. 25 (2016) 025009 (9pp) doi:10.1088/0964-1726/25/2/025009

Unimode metamaterials exhibiting negative linear compressibility and negative thermal expansion

Krzysztof K Dudek[1], Daphne Attard[1], Roberto Caruana-Gauci[1], Krzysztof W Wojciechowski[2] and Joseph N Grima[1,3]

[1] Metamaterials Unit, Faculty of Science, University of Malta, Msida MSD 2080, Malta
[2] Institute of Molecular Physics, Polish Academy of Sciences, M. Smoluchowskiego 17, 60-179, Poznań, Poland
[3] Department of Chemistry, Faculty of Science, University of Malta, Msida MSD 2080, Malta

E-mail: joseph.grima@um.edu.mt

Received 30 September 2015, revised 12 November 2015
Accepted for publication 16 November 2015
Published 4 January 2016

Abstract

Unimode metamaterials made from rotating rigid triangles are analysed mathematically for their mechanical and thermal expansion properties. It is shown that these unimode systems exhibit positive Poisson's ratios irrespective of size, shape and angle of aperture, with the Poisson's ratio exhibiting giant values for certain conformations. When the Poisson's ratio in one loading direction is larger than +1, the systems were found to exhibit the anomalous property of negative linear compressibility along this direction, that is, the systems expand in this direction when hydrostatically compressed. Also discussed are the thermal expansion properties of these systems under the assumption that the units exhibit increased rotational agitation once subjected to an increase in temperature. The effect of the geometric parameters on the aforementioned thermo-mechanical properties of the system, are discussed, with the aim of identifying negative behaviour.

S Online supplementary data available from stacks.iop.org/SMS/25/025009/mmedia

Keywords: negative compressibility, negative thermal expansion, rotating rigid units, analytical methods, Poisson's ratio

(Some figures may appear in colour only in the online journal)

1. Introduction

The last years have seen significant advancements in the field of mechanical metamaterials, that is, engineered systems that exhibit mechanical macroscopic properties that emerge due to the structure of their sub-units rather than their materials composition [1]. This class of systems intersects with other classes of systems which are becoming increasingly more studied, including auxetics [2] i.e. systems which exhibit a negative Poisson's ratio (NPR) as well as systems which exhibit negative linear compressibility (NLC) i.e. expand rather than shrink in at least one direction upon the application of a compressive hydrostatic pressure [3–13] and ones which contract in at least one direction when heated negative thermal expansion (NTE)[4] [14–29].

An interesting class of model systems which exhibit NPR are those built from connected sub-units which contain rigid units that rotate relative to each other upon the application of a uniaxial load [30–33]. These systems are

[4] Obviously, it must be noted that not all NPR, NLC and NTE materials are metamaterials and vice versa. For systems with such anomalous properties to be considered as metamaterials (or mechanical metamaterials so as to distinguish them from a wider class of metamaterials such as those which exhibit negative refractive indices, etc) they must be man-made, i.e. excluding materials such as zeolites or silicates which are naturally occurring.

rather easy to construct at various scales of structure ranging from the macro-scale level, for example through the use of perforations [34, 35] or pin-jointed structures, to the nanoscale, for example as zeolites or silicates [36–38]. It has been shown that for such systems to exhibit NPR, it is not enough that the rigid units within the system rotate relative to each other as these systems must also have amenable shapes and connectivities which lead to NPR. For example, it has been demonstrated that depending on the connectivity, 2D systems made from rotating rectangles of dimensions $a \times b$ can exhibit either an isotropic Poisson ratio of -1, or Poisson's ratios which are highly strain dependent and also depend on the direction of loading [30]. In the latter case, it was also shown that such systems can exhibit a positive Poisson's ratio which can be high. It was recently shown that highly positive Poisson's ratio can also give rise to NLC [39]. All this is very significant as systems which are describable in terms of rotating rigid units are commonly found in nature.

In addition to this, it has been shown that nano-systems based on rotating rigid units may also generate NTE [14, 15]. NTE manifests itself in shrinkage of the system, in at least one direction when subjected to an increase in temperature, as opposed to positive thermal expansion (PTE) which is characterised by an increase in at least one of the dimensions. One of the mechanisms leading to NTE in systems involves rigid unit behaviour and is akin to the mechanism giving rise to NPR. In this mechanism, formally known as rigid unit modes (RUMs), thermal excitation of low frequency phonon modes leads to a rocking type of motion of rigid units about a fully open configuration, resulting in a subsequent shrinkage in the unit cell.

Materials that exhibit NTE include polymers and other organic-based compounds [16–18], metal oxides [19–24], zeolites [25–27] and metal organic frameworks [28, 29]. In a number of these materials, the RUM mechanism plays a key role in their NTE behaviour. NTE materials are particularly interesting due to their possibility of being used to manufacture systems with tailored coefficients of thermal expansion. By combining them with PTE materials, one may achieve systems with tuned thermal properties such as systems with an overall zero thermal expansion. In this respect, it should be mentioned that a number of structures made from PTE materials that can have their thermal expansion tuned to negative, and even zero coefficients of thermal expansion, have also been designed [40, 41]. These include, amongst others, structures based on chiral honeycombs made from bi-material strips [40–42] and structures based on triangular units [43, 44]. It has also been shown that composite systems made of different PTE materials can be designed to exhibit NTE [45, 46].

Milton proposed and generalised various periodic unimode structures (structures that have a single easy mode of deformation [47]) built from rigid bars and pivots [48, 49], including ones built from connected triangles which behave as rotating rigid units [48]. One such system can be described through a sub-structure composed of four triangles which are connected together. Milton regards this structure, which should not be confused with other triangular lattices and geometries which have been extensively studied [31, 32, 50–55], as an expander since an application of a small strain in one direction may result in a considerable enhancement of the strain in the orthogonal direction [48]. In fact, it may be shown that such a structure may lead to very high positive Poisson's ratios in particular directions (see supplementary information available at stacks.iop.org/SMS/25/025009/mmedia), which as discussed in this work may in turn give rise to NLC.

Milton's work has clearly confirmed that the systems he considers exhibit high expandability. However, generalised mathematical models describing the mechanical behaviour of these systems and similar ones have not yet been established in terms of geometry. In this respect, it would be useful to develop a model which can quantify not only the expandability and expected Poisson's ratios of such systems but also other thermo-mechanical properties, such as thermal expansion or compressibility properties, which could also be of interest.

In view of this, and the important role that the relative rotation of rigid units has in generating anomalous thermo-mechanical properties, this work will look into more general systems which could be potentially constructed from Milton's expander, with the aim of formulating analytical models which can predict the Poisson's ratios, compressibility properties and thermal expansion behaviour of such constructs.

2. The model

Before examining the mechanical properties of these systems, it is useful to discuss their geometries, which are essentially generalisations and variations of Milton's expanders implemented as tessellations. One can establish a basic unit cell for such networks, consisting of two sets of two non-equivalent scalene triangles, as illustrated in figure 1(a). In such a case the shape of the system is describable through seven independent geometric parameters, six of which relate to the shape of the triangles of dimensions of $a \times b \times c$ and $d \times e \times f$ and one which relates to the degree of aperture of the system, angle θ. If one assumes that the triangles are rigid constructs, then the shape and size of this system rely on only one degree of freedom, the angle of aperture, thus qualifying it as a unimode system.

In this paper, we shall study a simpler case, where we only consider one type of triangle making up the unit cell. The sides of the triangle are denoted as a, b and c which subsequently define the interior angles of the triangle α, β and γ. The angle of aperture is defined by the angle θ which is twice the angle subtended between the side of length a and

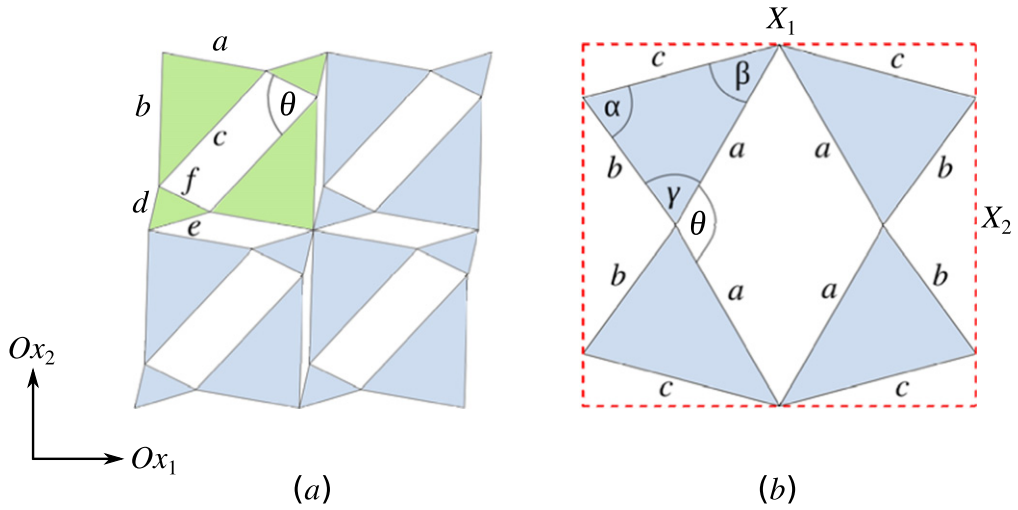

Figure 1. (a) A generalised structure based on Milton's expanders (b) the unit cell of a typical form of the systems studied here.

the Ox_1 direction. The triangles are connected in such a manner that sides of the same length make up the perimeter of the resulting pores (see figure 1(b)). Typically a triangle has all three vertices connected resulting in pores which are rhombic in shape. However there are some cases, in which the triangle has only two connections leaving a free vertex and as a consequence of this, a more complex pore shape is observed. The resulting unit cell always has two lines of symmetry (see supplementary information available at stacks.iop.org/SMS/25/025009/mmedia).

For a given triangle the system may be connected together in a tessellatable manner in a number of ways, henceforth referred to as forms. As a result of the geometry, although the different forms are very similar to each other, it is not possible to move from one form to another without permitting overlap of the triangles which *de facto* means that systems would be constrained to exist in only one of these forms unless the system is dismantled and re-assembled (see animation in supplementary information available at stacks.iop.org/SMS/25/025009/mmedia). In other words, depending on the value of θ and the dimensions $a \times b \times c$, only one of the six forms is permissible, i.e. a form may only exist in a bound range of angles, whose limits are henceforth referred to as transition angles θ^*. The transition angles occur whenever one of the three pores in the unit cell assumes a fully closed position. Since each pore has two different closed configurations, a total of six transition angles occur. These transition angles for $0^\circ \leqslant \theta^* \leqslant 360^\circ$ are a function of the interior angles of the triangle and are given by;

$$\theta^* \in \{2\beta,\ 180^\circ - 2\gamma,\ 180^\circ,\ 180^\circ + 2\beta,\ 360^\circ - 2\gamma,\ 360^\circ\}. \tag{1}$$

Note that the order of occurrence of the transition angles is not always the same and is dependent on the parameters describing the shape of the triangle. As a consequence of this, it is a futile exercise to name the different forms occurring for a general case of $a \times b \times c$.

The dimensions of the unit cell are also a function of the parameters a, b, c and θ and can be expressed as[5];

$$X_1 = 2\left(\max\left[0,\ a\cos\left(\frac{\theta}{2}\right),\ b\cos\left(\gamma+\frac{\theta}{2}\right)\right] - \min\left[0,\ a\cos\left(\frac{\theta}{2}\right),\ b\cos\left(\gamma+\frac{\theta}{2}\right)\right]\right), \tag{2}$$

$$X_2 = 2\left(\max\left[0,\ a\sin\left(\frac{\theta}{2}\right),\ b\sin\left(\gamma+\frac{\theta}{2}\right)\right] - \min\left[0,\ a\sin\left(\frac{\theta}{2}\right),\ b\sin\left(\gamma+\frac{\theta}{2}\right)\right]\right). \tag{3}$$

2.1. Mechanical properties

Using the obtained expressions for the dimensions of the unit cell, following the methodology discussed elsewhere [30–33, 53, 56, 57], one can then calculate the Poisson's ratio for each form using;

$$\nu_{12} = \frac{1}{\nu_{21}} = -\frac{\varepsilon_2}{\varepsilon_1} = -\frac{X_1}{X_2}\left(\frac{\mathrm{d}X_2}{\mathrm{d}\theta}\right)\cdot\left(\frac{\mathrm{d}X_1}{\mathrm{d}\theta}\right)^{-1}. \tag{4}$$

The Young's moduli, assuming a unit thickness z (where z is of the same order of magnitude of the parameters a, b and c), can be obtained using an energy approach. If the unit cell has an overall stiffness of K_h (which relates to the work required to change the angle of aperture) then the strain energy stored

[5] Equations (2) and (3) were obtained by considering a single triangle from the unit cell, calculating the co-ordinates of each of its vertices when the side a is aligned horizontally and then performing a rotation transformation by an angle $(\theta/2)$ to get the co-ordinates of the triangle when the degree of aperture of the system is θ. By subtracting the minimum X and Y co-ordinates from the maximum co-ordinates one can find the dimensions of the unit cell (an example concerning the dimensions of the unit-cell can be found in the supplementary information available at stacks.iop.org/SMS/25/025009/mmedia).

per unit cell, U is given by:

$$U = \frac{K_h}{2X_1X_2z}(\mathrm{d}\theta)^2. \tag{5}$$

The Young's modulus is related to the strain energy by:

$$E_i = \frac{2U}{{\varepsilon_i}^2} = K_h\frac{{X_i}^2}{X_1X_2z}\left(\frac{\mathrm{d}X_i}{\mathrm{d}\theta}\right)^{-2} \quad \text{where } i = 1,\ 2. \tag{6}$$

One may also write expressions for the linear compressibilities along the Ox_1 and Ox_2 directions [3] in terms of the Young's moduli and Poisson's ratios:

$$\beta_{\mathrm{L}}\left[Ox_1\right] = s_{11} + s_{12} = \frac{1}{E_1} - \frac{\nu_{21}}{E_2}, \tag{7}$$

$$\beta_{\mathrm{L}}\left[Ox_2\right] = s_{21} + s_{22} = \frac{1}{E_2} - \frac{\nu_{12}}{E_1}, \tag{8}$$

where s_{ij} are the compliance coefficients. The area compressibility can be found from the linear compressibilities through:

$$\beta_{\mathrm{A}} = \beta_{\mathrm{L}}\left[Ox_1\right] + \beta_{\mathrm{L}}\left[Ox_2\right]. \tag{9}$$

2.2. Thermal properties

Apart from the mechanical properties of the model under consideration, one could also investigate the thermal expansion properties of the presented system, based on the work on RUMs which has already been done in the field of thermal expansion [15, 58–60]. If the system is in a conformation having a maximum area when in its cold state (corresponding to the temperature in the vicinity of 0 K), where the angle between the units is $\theta = \theta_0$, then it is possible for it to exhibit a NTE upon heating as the units vibrate with an amplitude of $\Delta\theta$ about θ_0.

To simplify the analysis, based on previous work [15, 61], the following assumptions will be made, namely that (i) the units are rigid so that the only mode of deformation is through rotation; (ii) the rigid units behave as harmonic oscillators so that the thermal average of $\Delta\theta$ at a given temperature T, i.e. $\langle\Delta\theta\rangle_T$ is zero; (iii) the amplitude of oscillations is small so as to allow for small angle approximations for terms involving $\Delta\theta$.

For the sake of simplicity, systems constructed from isosceles triangles with $b = c > a$ shall be used as an example to illustrate this NTE effect. For such a case, as discussed in further detail in the discussion, the form which occurs in the range of $180^\circ - 2\gamma < \theta < 2\beta$ is one of the most predominant forms and also has the maximum area for the system. For such a form, the unit cell dimensions can be expressed by means of the following equations:

$$X_1 = a\cos\left(\frac{\theta}{2}\right) - b\cos\left(\gamma + \frac{\theta}{2}\right), \tag{10}$$

$$X_2 = b\sin\left(\gamma + \frac{\theta}{2}\right). \tag{11}$$

Thus the area of the unit-cell may be defined as a product of the above quantities, hence:

$$A(\theta) = X_1(\theta)\cdot X_2(\theta) = b\left(a\cos\left(\frac{\theta}{2}\right)\right.$$
$$\left.\times\sin\left(\gamma + \frac{\theta}{2}\right) - b\cos\left(\gamma + \frac{\theta}{2}\right)\sin\left(\gamma + \frac{\theta}{2}\right)\right). \tag{12}$$

From this equation it can be shown that the maximum area of the unit-cell occurs at $\theta_0 = \frac{\pi}{2}$, about which point it is also symmetric such that $A(\theta_0 + \Delta\theta) = A(\theta_0 - \Delta\theta)$. Subsequently, the area can be expressed in terms of the equilibrium angle θ_0 and its change $\Delta\theta$ as follows:

$$\begin{aligned} A\left(\theta_0 + \Delta\theta\right) &= b\left[\frac{a}{2}\sin\left(\gamma + \frac{\pi}{2} + \Delta\theta\right) + \frac{a}{2}\sin\gamma\right. \\ &\quad \left. -\frac{b}{2}\sin\left(2\gamma + \frac{\pi}{2} + \Delta\theta\right)\right] \\ &= b\left[\frac{a}{2}(\cos\gamma\cos\Delta\theta\right. \\ &\quad -\sin\gamma\sin\Delta\theta) + \frac{a}{2}\sin\gamma \\ &\quad -\frac{b}{2}(\cos 2\gamma\cos\Delta\theta \\ &\quad \left.-\sin 2\gamma\sin\Delta\theta)\right]. \end{aligned} \tag{13}$$

Assuming the change in angle, $\Delta\theta$, is small, this equation can be further simplified, using the Taylor series, so that the thermal average of the area can be expressed by:

$$\begin{aligned} \langle A\rangle_T = b\left[\frac{a}{2}\cos\gamma\left(1 - \frac{\left\langle\Delta\theta^2\right\rangle_T}{2}\right) + \frac{a}{2}\sin\gamma\right. \\ \left. -\frac{b}{2}\cos 2\gamma\left(1 - \frac{\left\langle\Delta\theta^2\right\rangle_T}{2}\right)\right]. \end{aligned} \tag{14}$$

In order to express $\left\langle\Delta\theta^2\right\rangle_T$ in terms of the temperature T one could use the approach proposed in [15] which is based on the principle of the equipartition of the energy, which states that every mode, of which there is only one in this case, is provided with the energy equal to $\frac{1}{2}k_{\mathrm{B}}T$, where k_{B} is the Boltzmann constant (1.38×10^{-23} J K^{-1}). Thus:

$$\frac{1}{2}I\omega^2\left\langle\Delta\theta^2\right\rangle_T = \frac{1}{2}k_{\mathrm{B}}T, \tag{15}$$

where I is the moment of inertia of the rotating rigid units and ω is the frequency by which the units oscillate. This gives a thermal expansion coefficient α_{A} of:

$$\alpha_{\mathrm{A}} = \frac{1}{\langle A\rangle_T}\left(\frac{\mathrm{d}\langle A\rangle_T}{\mathrm{d}T}\right)_p = \frac{k_{\mathrm{B}}(b\cos(2\gamma) - a\cos(\gamma))}{2aI\omega^2\sin(\gamma) + a\left(2I\omega^2 - k_{\mathrm{B}}T\right)\cos(\gamma) - b\left(2I\omega^2 - k_{\mathrm{B}}T\right)\cos(2\gamma)}. \tag{16}$$

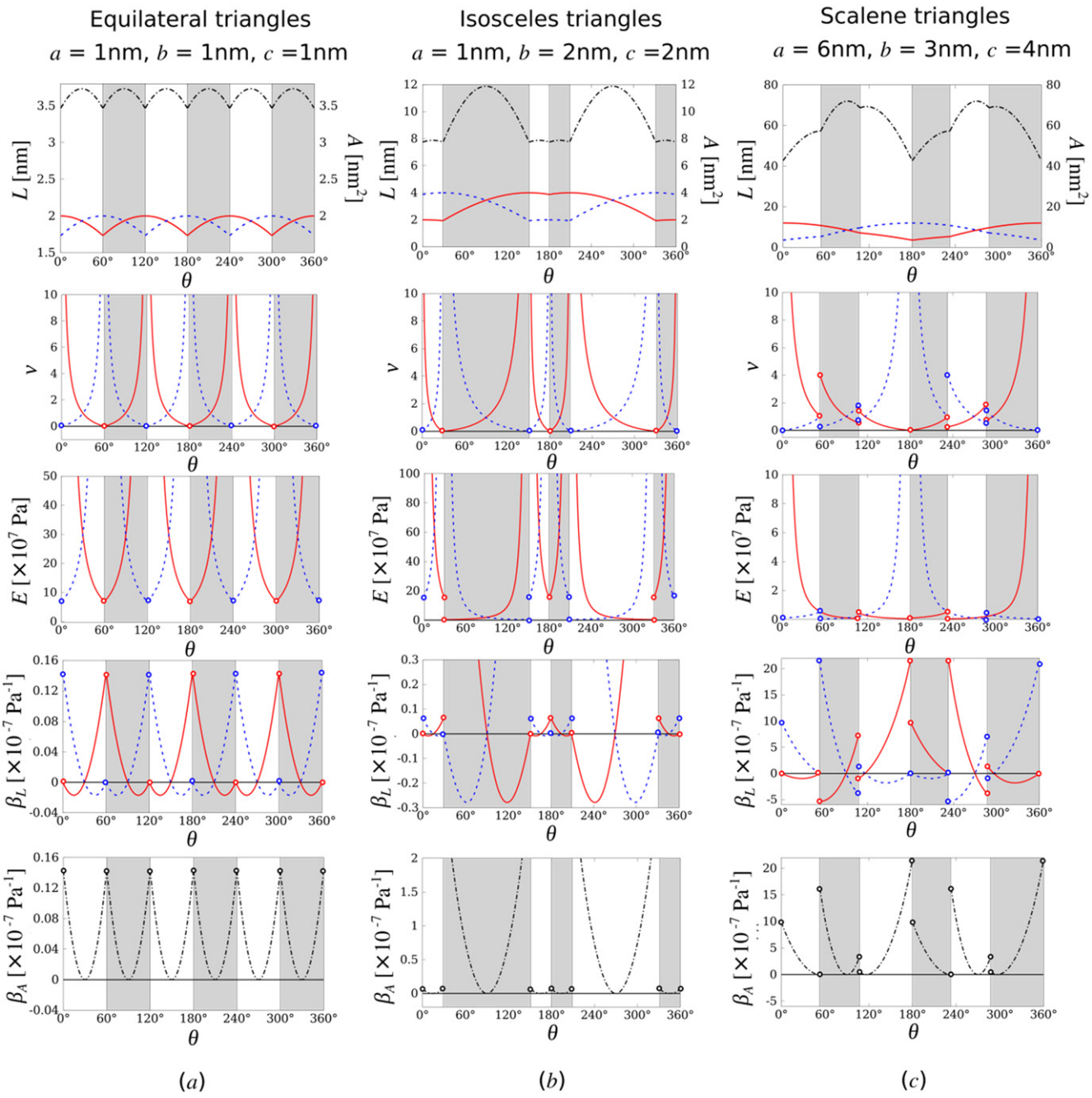

Figure 2. Graphs for the unit cell dimensions and mechanical properties of three different systems constructed from (a) equilateral (b) isosceles and (c) scalene triangles. The red lines represent the behaviour of the quantities associated with the Ox_1 direction, the blue lines correspond to the Ox_2 direction whereas the black lines correspond to the area. The different shade of the background of the graphs is used to distinguish the different forms exhibited by the system. The stiffness constant K_h was set to be 12 kJ mol^{-1} rad^{-2}.

3. Results and discussion

Plots for the dimensions and mechanical properties of three particular cases of triangles (equilateral, isosceles and scalene) are presented in figure 2. The plots are divided into regions corresponding to different forms of the triangles (diagrams representing these three types of triangles and their respective forms and transitions can be found in the supplementary information available at stacks.iop.org/SMS/25/025009/mmedia). It is evident that on changing the geometry of the triangle, the mechanical properties change accordingly. However, before discussing the actual mechanical properties of the systems, it is useful to first discuss the constructability or otherwise of these systems, i.e. the number of forms that such systems can have and the angle range over which these forms occur. This will be followed by a discussion of thermo-mechanical properties afforded by these systems.

Looking at the constructability of these systems, it should be noted that the range of angles over which the different forms occur changes with the shape of the triangle, even

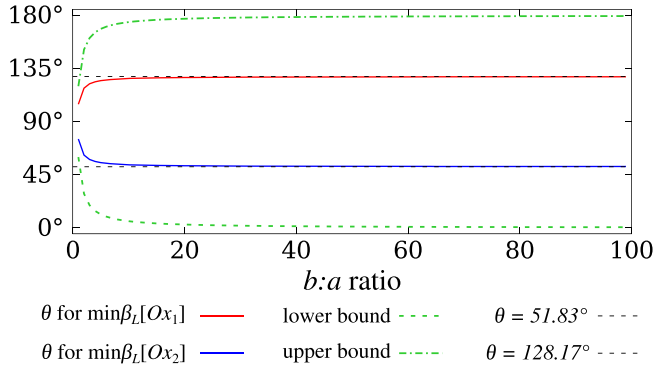

Figure 3. Variation of the range of angles in which NLC is exhibited for a particular form on changing the *b:a* ratio of an isosceles triangle.

though there are always six of such forms. For an equilateral triangle, all six forms will each have a range of 60°, whilst for an isosceles triangle, four forms will have the same extent of range and two forms will have the same extent of range, which range is different from the other four forms. On the other hand, a scalene triangle will have three pairs of forms where each pair has the same extent of range, which extent is different from that of other pairs. This pairing up of forms occurs since these forms are a 90° rotation of each other. Thus on considering all types of triangles, it becomes evident that the change in the extent of the ranges is related to the ratio of the sides of the triangles. On increasing the disparity of the sides (and hence changing their ratio), the extent of the ranges changes accordingly. This can be observed, especially for isosceles triangles, from figures 2 and 3. This kind of behaviour is reflected in all the mechanical properties of the systems. It must be mentioned that if one were to increase the sides of the triangle in such a manner so as to keep the same ratio, the extent of the ranges will remain unchanged but the magnitude of the mechanical properties is affected except for the Poisson's ratio since this is scale independent.

In terms of the mechanical properties, a look at the plots shown in figure 2 will reveal that the mechanical properties afforded by the systems are highly dependent on the form in which the system exists, with a marked discontinuity in the mechanical properties between one region and the next. This is because at the transition angles, the forms are in a locked conformation and hence the mechanical properties at that particular angle cannot be defined. This is in contrast to the behaviour of the unit cell dimensions which are characterised by a continuous transition from one form to the next. This implies that at the transition angles, both forms have the same dimensions.

On examining the Poisson's ratio for all three different types of triangles presented, it is evident that the Poisson's ratio is positive for all values of θ and can have large values, i.e. there is no auxetic behaviour. These large values tend to occur when the derivative of the dimension along which the system is being loaded tends to zero. In the case of the equilateral and isosceles triangles, such behaviour is observed at the vicinity of each transition angle. A similar behaviour is also observed for the Young's moduli.

It is also evident from the plots in figure 2 that all the systems considered exhibit NLC. In fact, for the whole range of θ-values the systems exhibit NLC along Ox_1 or Ox_2 but never in both directions simultaneously. This ensures that the area compressibility β_A is never negative, so that on application of a hydrostatic pressure, the area of the system always decreases, resulting in densification of the system, even though one-dimension may increase in size. Thus the 2D equivalent of the bulk modulus of these systems is always positive. It is interesting to note that the total range over which NLC is observed along the Ox_1 direction is equal to that over which NLC is observed along the Ox_2 direction. In other words, NLC is observed in the Ox_1 and Ox_2 over a total range of almost 180° for each direction (except for values at the transition angles, at which values, compressibility is undefined).

On further examination of the plots, it can be observed that for each form, the range in which NLC occurs is bound. The bounds correspond to the instance where the unit cell of that form has a maximum area and by the instance when the form is fully opened in one of its major axis which occurs at the transition angle. When the area of a form is close to its maximum, applying a hydrostatic pressure causes it to decrease. Since the Poisson's ratio of the system is positive for all angles, then on application of a hydrostatic pressure, one of the unit cell dimension increases in length exhibiting NLC whilst the other unit cell dimension decreases in length, exhibiting positive linear compressibility. This effect is observed until the unit cell dimension which is increasing in length achieves a fully extended position, at which point the transition angle would have been reached.

Another way of describing the range in which NLC is observed is through the Poisson's ratios. It can be shown that in cases where deformation occurs through a unimode hinging mechanism, as in the systems described here, typically, the Poisson's ratio fulfils the relation $\nu_{12} = (\nu_{21})^{-1}$. In such cases, it follows from equations (4) and (6) that the occurrence of NLC along Ox_1 direction (equation (7)) can be expressed by the requirement that the strains along the Ox_1 and Ox_2 directions, ε_1 and ε_2 respectively, must satisfy the condition ${\varepsilon_1}^2 + \varepsilon_1\varepsilon_2 < 0$, i.e. $\varepsilon_1\varepsilon_2 < 0$ and $|\varepsilon_1\varepsilon_2| > {\varepsilon_1}^2$. This condition is satisfied whenever $|\varepsilon_2| > |\varepsilon_1|$ and the Poisson's ratios are positive (see supplementary information for a detailed derivation available at stacks.iop.org/SMS/25/025009/mmedia). Thus, when $\nu_{12} > +1$, $\beta_L[Ox_1] < 0$. In a more general manner, this means that whenever one of the Poisson's ratios for loading in one direction is greater than +1 (and hence larger than the Poisson's ratio for loading along the other direction because of their inverse relation), NLC is observed in that direction.

It should also be mentioned here that the magnitude of NLC is affected by the shape and size of the triangles. Considering an isosceles triangle ($b = c$) for the sake of simplicity (but similar arguments may also hold for scalene triangles), on increasing the sides but keeping the same aspect ratio, the magnitude of the compressibilities increases accordingly, while the range over which NLC is exhibited for

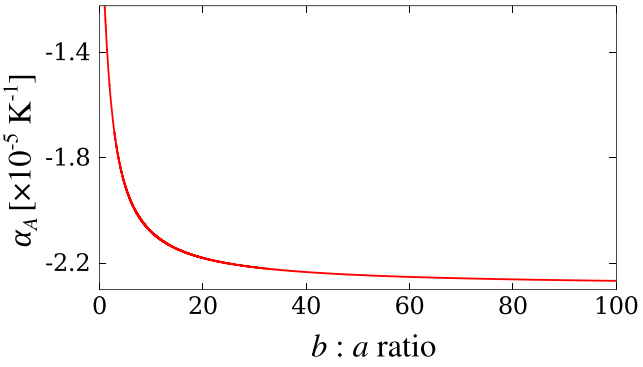

Figure 4. Variation of the thermal expansion coefficient with the aspect ratio of isosceles triangles for systems where $b = c > a = 1$ having a form that exists for $180° - 2\gamma < \theta < 2\beta$ and vibrating about an equilibrium angle of 90°. The temperature was set to be equal to $T = 293$ K and the value of $I\omega^2$ was set to be equal to $75k_BT$.

a particular form remains unchanged. On the other hand, if the b:a ratio of the isosceles triangles increases from 1, NLC values become more negative and one of the forms becomes increasingly more predominant. In the limit that this ratio approaches infinity, when virtually only one form is possible, the triangles become flattened to a line, and geometry wise, the structure becomes similar to a wine-rack. As illustrated in figure 3, on increasing the b:a ratio, the angles at which the most NLC values occur tend to that of 128.17° or 51.83° (corresponding to $\beta_L[Ox_1]$ and $\beta_L[Ox_2]$ respectively) which angles are identical to that at which the wine-rack-type mechanism exhibits minimum (most negative) linear compressibility [39, 62]. These angles do not seem to have any particular geometrical significance but are obtained on solving for the minimum compressibilities. In fact, in the particular cases where $b > a$, the form with the widest extent of range and which exhibits the most negative values for linear compressibility has the cell parameters:

$$X_1 = 2a\cos\left(\frac{\theta}{2}\right) - 2b\cos\left(\gamma + \frac{\theta}{2}\right), \tag{17}$$

$$X_2 = 2b\sin\left(\gamma + \frac{\theta}{2}\right). \tag{18}$$

In the limit that $b \gg a$, $\gamma \to 90°$ and hence equations (17) and (18) may be expressed by:

$$X_1 \approx 2b\sin\left(\frac{\theta}{2}\right), \tag{19}$$

$$X_2 \approx 2b\cos\left(\frac{\theta}{2}\right) \tag{20}$$

which equations correspond to that of the wine-rack-like [39] structure after recognising the differences in orientation.

In terms of the thermal expansion properties, the equations derived above, particularly equation (16) suggests that the system presented here may also exhibit NTE, that is, it decreases in size along one or more directions on the application of heat. From the plots of the unit-cell parameters (see figure 2) it is evident that at certain angles of aperture the unit-cell has a maximum area. If on heating, the system oscillates about a point of maximum area configuration *via* a 'RUM', as discussed in various works [15, 58–61] its area will decrease. This is of particular significance as it suggests that the presented system may exhibit both NLC and NTE.

Moreover, as evident from equation (16), the magnitude of the coefficient of thermal expansion is dependent on the shape of the isosceles triangles, i.e. on the ratio of the side dimensions. This is illustrated more clearly in figure 4 which shows how the coefficient of thermal expansion for a system of isosceles triangles vibrating about an equilibrium angle of 90° (which angle, as illustrated in figure 2, is a point of maximum area) changes with the shape of the isosceles triangles. In the cases considered the temperature was set to be equal to $T = 293$ K and the value of $I\omega^2$ was set to be equal to $75k_BT$. In general the dimensions of the triangular units could be assigned arbitrary values in the nano-scale. In these cases the value of a was kept constant at 0.5 nm whilst the lengths of sides b and c were increased up to 50 nm in steps of 0.001 nm. The plot in figure 4 suggests that, in this case, the magnitude of NTE increases as the triangles become more slender, as was the case for the compressibility. Here, it should be highlighted that the plot only represents one of the six forms in which the system can exist. There may be other forms which also give rise to NTE, albeit to a different extent, as is clear from the plot of area against θ in figure 2, where for any type of triangle, more than one area maximum occur.

All this is very significant because the system studied here can be used as a blueprint to design materials that not only have NLC but also NTE concurrently. Also significant is the finding made through this work that although networks constructed from rotating rigid triangles are usually closely associated with auxeticity, this may not always be the case as clearly illustrated by the systems considered here which instead can exhibit giant positive Poisson's ratio properties which are conducive to NLC. This highlights the versatility of these systems which when designed in a specific geometric conformation have the potential to exhibit tailored negative properties. Possible applications for systems which exhibit NLC include their use in high pressure environments and as sensitive interferometric pressure sensors [3]. NTE materials are sought for their use in obtaining composites with tailored coefficients of thermal expansion. Such composites could be used in a variety of ways ranging from dental fillings [63] to solar arrays in telescopes [64] and other applications which involve large fluctuations in temperature that could lead to thermal cracking.

Before concluding one should mention that although *a prima facie* both equations describing the compressibility and thermal expansion of the systems seem to be only dependent on the ratios of the sides of the triangles, the NLC and NTE effects described here are likely to manifest themselves only if the system is at a molecular scale. For the thermal expansion analysis described here to apply, the structural features must be small enough for thermal vibrational motion to be present. One would not expect such thermal vibrations, and hence

such a mechanism, to occur on a macro-scale structure. Similarly, the mechanism responsible for NLC in the model presented here is such that the hydrostatic pressure is only exerted on the outside of the system, that is, the fluid particles exerting the hydrostatic pressure on the system should not permeate through the system (as discussed in [39]). Thus it may be difficult for such a mechanism to operate at a macro-scale, however, it may manifest itself at a nano level, providing the material has the necessary geometric features which allow this mechanism to occur, which ideally is also the only mechanism of deformation. Other modes of deformation acting concurrently with the hinging mechanism may in fact diminish the effect of NLC where it exists [39], although, they may themselves cause NLC in particular directions to be exhibited over a larger range of angles as highlighted in previous work [65].

4. Conclusion

It has been shown through analytical modelling that systems based on the Milton's unimode expanders can occur in various forms depending on the shape of the triangles and the angle of aperture. It has been found that these systems have an excellent potential for exhibiting NLC along particular directions, a property resulting from the very high positive Poisson's ratio that these systems can exhibit. It has also been shown how the size and shape of triangles affect the magnitude and range of NLC for a particular form, even though the overall range of NLC along each direction remains constant. The magnitude of NLC was found to increase on increasing the ratio of the sides of the triangles, with maximum NLC characteristics being exhibited when the geometry of system and the deformation profile approach that of the well-known wine-rack-like mechanism. It has also been suggested that such unimode metamaterials, under the standard assumptions made for similar RUM systems, may exhibit NTE, whose magnitude also seems to get larger the more slender the triangles are.

Given the significance of this work, it is hoped that the findings obtained here will provide an impetus for further studies in the field of mechanical metamaterials and other systems with negative properties.

References

[1] Grima J N and Caruana-Gauci R 2012 Mechanical metamaterials: materials that push back *Nat. Mater.* **11** 565–6

[2] Evans K E, Nkansah M A, Hutchinson I J and Rogers S 1991 Molecular network design *Nature* **353** 124

[3] Baughman R H, Stafstrom S, Cui C and Dantas S O 1998 Materials with negative compressibilities in one or more dimensions *Science* **279** 1522–4

[4] Serra-Crespo P, Dikhtiarenko A, Stavitski E, Juan-Alcañiz J, Kapteijn F, Coudert F-X and Gascon J 2014 Experimental evidence of negative linear compressibility in the MIL-53 metal–organic framework family *CrystEngComm* **17** 276–80

[5] Weng C N, Wang K T and Chen T 2008 Design of microstructures and structures with negative linear compressibility in certain directions *Adv. Mater. Res.* **33–37** 807–14

[6] Cairns A B, Catafesta J, Levelut C, Rouquette J, van der Lee A, Peters L, Thompson A L, Dmitriev V, Haines J and Goodwin A L 2013 Giant negative linear compressibility in zinc dicyanoaurate *Nat. Mater.* **12** 212–6

[7] Goodwin A L, Keen D A and Tucker M G 2008 Large negative linear compressibility of $Ag_3[Co(CN)_6]$ *Proc. Natl Acad. Sci. USA* **105** 18708–13

[8] Barnes D L, Miller W, Evans K E and Marmier A 2012 Modelling negative linear compressibility in tetragonal beam structures *Mech. Mater.* **46** 123–8

[9] Fortes A D, Suard E and Knight K S 2011 Negative linear compressibility and massive anisotropic thermal expansion in methanol monohydrate *Science* **331** 742–6

[10] Li W, Probert M R, Kosa M, Bennett T D, Thirumurugan A, Burwood R P, Parinello M, Howard J A K and Cheetham A K 2012 Negative linear compressibility of a metal–organic framework *J. Am. Chem. Soc.* **134** 11940–3

[11] Coudert F-X 2013 Systematic investigation of the mechanical properties of pure silica zeolites: stiffness, anisotropy, and negative linear compressibility *Phys. Chem. Chem. Phys.* **15** 16012–8

[12] Cairns A B and Goodwin A L 2015 Negative linear compressibility *Phys. Chem. Chem. Phys.* **17** 20449–65

[13] Cairns A B, Thompson A L, Tucker M G, Haines J and Goodwin A L 2012 Rational design of materials with extreme negative compressibility: selective soft-mode frustration in $KMn[Ag(CN)_2]_3$ *J. Am. Chem. Soc.* **134** 4454–6

[14] White M A 2011 *Physical Properties of Materials* (Boca Raton, FL: CRC Press)

[15] Welche P R L, Heine V and Dove M T 1998 Negative thermal expansion in beta-quartz *Phys. Chem. Miner.* **26** 63–77

[16] Bruno J, Allan N, Barron T and Turner A 1998 Thermal expansion of polymers: mechanisms in orthorhombic polyethylene *Phys. Rev.* B **58** 8416–27

[17] Mukherjee M, Bhattacharya M, Sanyal M K, Geue T, Grenzer J and Pietsch U 2002 Reversible negative thermal expansion of polymer films *Phys. Rev.* E **66** 061801

[18] Wang K-Y, Feng M-L, Zhou L-J, Li J-R, Qi X-H and Huang X-Y 2014 A hybrid with uniaxial negative thermal expansion behaviour: the synergistic role of organic and inorganic components *Chem. Commun.* **50** 14960–3

[19] Mary T A, Evans J S O, Vogt T and Sleight A W 1996 Negative thermal expansion from 0.3 to 1050 Kelvin in ZrW_2O_8 *Science* **272** 90–2

[20] Pryde A K A, Dove M T and Heine V 1999 Simulation studies of ZrW_2O_8 at high pressure *J. Phys.: Condens. Matter* **10** 8417–28

[21] Evans J S O, Mary T A and Sleight A W 1997 Negative thermal expansion materials *Physica* B **241–243** 311–6

[22] Amos T G and Sleight A W 2001 Negative thermal expansion in orthorhombic $NbOPO_4$ *J. Solid State Chem.* **160** 230–8

[23] Barrera G D, Bruno J A O, Barron T H K and Allan N L 2005 Negative thermal expansion *J. Phys.: Condens. Matter* **17** R217–52

[24] Romao C P, Miller K J, Johnson M B, Zwanziger J W, Marinkovic B A and White M A 2014 Thermal, vibrational, and thermoelastic properties of $Y_2Mo_3O_{12}$ *Phys. Rev.* B **90** 024305

[25] Lightfoot P, Woodcock D A, Maple M J, Villaescusa L A and Wright P A 2001 The widespread occurrence of negative thermal expansion in zeolites *J. Mater. Chem.* **11** 212–6

[26] Marinkovic B A, Jardim P M, Rizzo F, Saavedra A, Lau L Y and Suard E 2008 Complex thermal expansion properties of Al-containing HZSM-5 zeolite: a x-ray

diffraction, neutron diffraction and thermogravimetry study *Microporous Mesoporous Mater.* **111** 110–6
[27] Fang H and Dove M T 2013 Pressure-induced softening as a common feature of framework structures with negative thermal expansion *Phys. Rev.* B **87** 214109
[28] Rimmer L H N, Dove M T, Winkler B, Wilson D J, Refson K and Goodwin A L 2014 Framework flexibility and the negative thermal expansion mechanism of copper(I) oxide Cu_2 O *Phys. Rev.* B **89** 214115
[29] Li H, Eddaoudi M, O'Keeffe M and Yaghi O M 1999 Design and synthesis of an exceptionally stable and highly porous metal–organic framework *Nature* **402** 276–9
[30] Grima J N, Gatt R, Alderson A and Evans K E 2005 On the auxetic properties of 'rotating rectangles' with different connectivity *J. Phys. Soc. Japan* **74** 2866–7
[31] Grima J N, Chetcuti E, Manicaro E, Attard D, Camilleri M, Gatt R and Evans K E 2012 On the auxetic properties of generic rotating rigid triangles *Proc. R. Soc.* A **468** 810–30
[32] Grima J N and Evans K E 2006 Auxetic behavior from rotating triangles *J. Mater. Sci.* **41** 3193–6
[33] Grima J N and Evans K E 2000 Auxetic behavior from rotating squares *J. Mater. Sci. Lett.* **19** 1563–5
[34] Grima J N and Gatt R 2010 Perforated sheets exhibiting negative Poisson's ratios *Adv. Eng. Mater.* **12** 460–4
[35] Bertoldi K, Reis P M, Willshaw S and Mullin T 2010 Negative Poisson's ratio behavior induced by an elastic instability *Adv. Mater.* **22** 361–6
[36] Lethbridge Z A D, Williams J J, Walton R I, Smith C W, Hooper R M and Evans K E 2006 Direct, static measurement of single-crystal Young's moduli of the zeolite natrolite: comparison with dynamic studies and simulations *Acta Mater.* **54** 2533–45
[37] Sanchez-Valle C, Lethbridge Z A D, Sinogeikin S V, Williams J J, Walton R I, Evans K E and Bass J D 2008 Negative Poisson's ratios in siliceous zeolite MFI-silicalite *J. Chem. Phys.* **128** 184503
[38] Grima J N, Gatt R, Alderson A and Evans K E 2006 An alternative explanation for the negative Poisson's ratios in alpha-cristobali *Mater. Sci. Eng.* A **423** 219–24
[39] Grima J N, Attard D, Caruana-Gauci R and Gatt R 2011 Negative linear compressibility of hexagonal honeycombs and related systems *Scr. Mater.* **65** 565–8
[40] Lakes R S 2007 Cellular solids with tunable positive or negative thermal expansion of unbounded magnitude *Appl. Phys. Lett.* **90** 221905
[41] Ha C S, Hestekin E, Li J, Plesha M E and Lakes R S 2015 Controllable thermal expansion of large magnitude in chiral negative Poisson's ratio lattices *Phys. Status Solidi* B **252** 1431–4
[42] Lakes R S 1996 Cellular solid structures with unbounded thermal expansion *J. Mater. Sci. Lett.* **15** 475–7
[43] Grima J N, Farrugia P-S, Gatt R and Zammit V 2007 A system with adjustable positive or negative thermal expansion *Proc. R. Soc.* A **463** 1585–96
[44] Lim T-C 2005 Anisotropic and negative thermal expansion behavior in a cellular microstructure *J. Mater. Sci.* **40** 3275–7
[45] Grima J N, Oliveri L, Ellul B, Gatt R, Attard D, Cicala G and Recca G 2010 Adjustable and negative thermal expansion from multilayered systems *Phys. Status Solidi—Rapid Res. Lett.* **4** 133–5
[46] Sigmund O and Torquato S 1996 Composites with extremal thermal expansion coefficients *Appl. Phys. Lett.* **69** 3203–5
[47] Milton G W and Cherkaev A V 1995 Which elasticity tensors are realizable? *J. Eng. Mater. Technol.* **117** 483–93
[48] Milton G W 2013 Complete characterization of the macroscopic deformations of periodic unimode metamaterials of rigid bars and pivots *J. Mech. Phys. Solids* **61** 1543–60
[49] Milton G W 2015 New examples of three-dimensional dilational materials *Phys. Status Solidi* B **252** 1426–30
[50] Hutchinson R G and Fleck N A 2006 The structural performance of the periodic truss *J. Mech. Phys. Solids* **54** 756–82
[51] Mitschke H, Robins V, Mecke K and Schröder-Turk G E 2012 Finite auxetic deformations of plane tessellations *Proc. R. Soc.* A **469** 20120465
[52] Mitschke H, Schröder-Turk G E, Mecke K, Fowler P W and Guest S D 2013 Symmetry detection of auxetic behaviour in 2D frameworks *EPL (Europhys. Lett.)* **102** 66005
[53] Kapko V, Treacy M M J, Thorpe M F and Guest S D 2009 On the collapse of locally isostatic networks *Proc. R. Soc.* A **465** 3517–30
[54] Larsen U, Sigmund O and Bouwstra S 1997 Design and fabrication of compliant micromechanisms and structures with negative Poisson's ratio *J. Microelectromech. Syst.* **6** 99–106
[55] Cabras L and Brun M 2014 Auxetic two-dimensional lattice with Poisson's ratio arbitrarily close to -1 *Proc. R. Soc.* A **470** 20140538
[56] Grima J N, Alderson A and Evans K E 2004 Negative Poisson's ratio from rotating rectangl *Comput. Methods Sci. Technol.* **10** 137–45
[57] Grima J N, Jackson R, Alderson A and Evans K E 2000 Do zeolites have negative Poisson's ratios? *Adv. Mater.* **12** 1912–8
[58] Tautz F S, Heine V, Dove M T and Chen X 1991 Rigid unit modes in the molecular dynamics simulation of quartz and the incommensurate phase transition *Phys. Chem. Miner.* **18** 326–36
[59] Pryde A K A, Hammonds K D, Dove M T, Heine V, Gale J D and Warren M C 1996 Origin of the negative thermal expansion in ZrW_2O_8 and ZrV_2O_7 *J. Phys.: Condens. Matter* **8** 10973–82
[60] Miller W, Smith C W, Mackenzie D S and Evans K E 2009 Negative thermal expansion: a review *J. Mater. Sci.* **44** 5441–51
[61] Grima J N, Bajada M, Scerri S, Attard D, Dudek K K and Gatt R 2015 Maximizing negative thermal expansion via rigid unit modes: a geometry-based approach *Proc. R. Soc.* A **471** 20150188
[62] Miller W, Evans K E and Marmier A 2015 Negative linear compressibility in common materials *Appl. Phys. Lett.* **106** 231903
[63] Versluis A, Douglas W H and Sakaguchi R L 1996 Thermal expansion coefficient of dental composites measured with strain gauges *Dent. Mater.* **12** 290–4
[64] Sigmund O and Torquato S 1997 Design of materials with extreme thermal expansion using a three-phase topology optimization method *J. Mech. Phys. Solids* **45** 1037–67
[65] Grima J N, Caruana-Gauci R, Wojciechowski K W and Evans K E 2013 Smart hexagonal truss systems exhibiting negative compressibility through constrained angle stretching *Smart Mater. Struct.* **22** 084015